RESEARCH ARTICLE | MAY 08 2023

Giant and broadband THz and IR emission in drift-biased graphene-based hyperbolic nanostructures *⊙*

L. Wang; N. K. Paul; J. Hihath; ... et. al



Appl. Phys. Lett. 122, 191703 (2023) https://doi.org/10.1063/5.0145288





CrossMark

Articles You May Be Interested In

Enhanced light-matter interactions at photonic magic-angle topological transitions

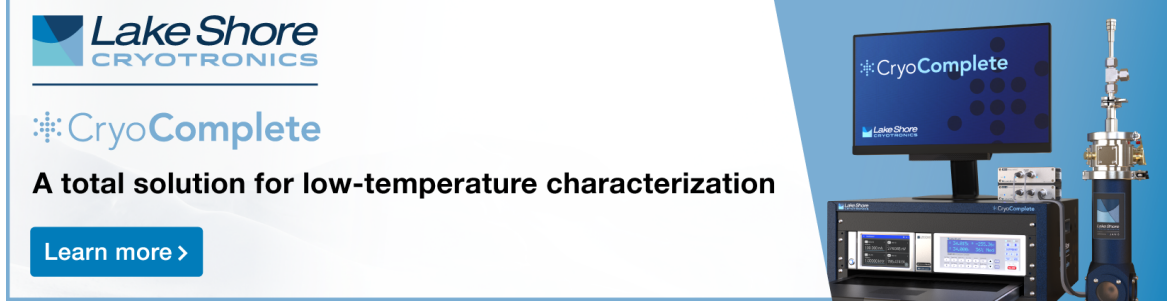
Appl. Phys. Lett. (May 2021)

Voltage-adjustable terahertz hyperbolic metamaterial based on graphene and doped silicon

AIP Advances (January 2019)

A terahertz Brewster switch based on superconductor hyperbolic metamaterial

Journal of Applied Physics (November 2020)





Giant and broadband THz and IR emission in drift-biased graphene-based hyperbolic nanostructures

Cite as: Appl. Phys. Lett. **122**, 191703 (2023); doi: 10.1063/5.0145288 Submitted: 4 February 2023 · Accepted: 24 April 2023 · Published Online: 8 May 2023







L. Wang, N. K. Paul, J. Hihath, and J. S. Gomez-Diaz, in

AFFILIATIONS

- ¹Department of Electrical and Computer Engineering, University of California Davis, One Shields Avenue, Kemper Hall 2039, Davis, California 95616, USA
- ²Biodesign Center for Bioelectronics and Biosensors, School of Electrical, Computer and Energy Engineering, Arizona State University, Tempe, Arizona 85287, USA

ABSTRACT

We demonstrate that Cherenkov radiation can be manipulated in terms of operation frequency, bandwidth, and efficiency by simultaneously controlling the properties of drifting electrons and the photonic states supported by their surrounding media. We analytically show that the radiation rate strongly depends on the momentum of the excited photonic state, in terms of magnitude, frequency dispersion, and its variation vs the properties of the drifting carriers. This approach is applied to design and realize miniaturized, broadband, tunable, and efficient terahertz and far-infrared sources by manipulating and boosting the coupling between drifting electrons and engineered hyperbolic modes in graphene-based nanostructures. The broadband, dispersive, and confined nature of hyperbolic modes relax momentum matching issues, avoid using electron beams, and drastically enhance the radiation rate—allowing that over 90% of drifting electrons emit photons. Our findings open an exciting paradigm for the development of solid-state terahertz and infrared sources.

Published under an exclusive license by AIP Publishing. https://doi.org/10.1063/5.0145288

The generation and control of electromagnetic waves have helped shape the development of our society. Approaches, such as thermal radiation (light bulbs), thermionic emission (vacuum tubes), stimulated emission (lasers), and electroluminescence (LEDs), have been incorporated into everyday technologies covering the realms of electronics and photonics. Between these two regimes lies the terahertz (THz) and far-infrared (IR) bands (~0.5-20 THz), which offer unique opportunities to enable communication systems with terabit per second data rates, ultra-fast and miniaturized processing systems, highresolution imaging for inspection and screening, and innumerable biomedical and sensing devices. Unfortunately, our society is not fully enjoying the benefits of these and other applications because the limited response of materials in this frequency band prevents efficient generation of THz and far-IR light in a simple and portable way. 1,5 Indeed, state-of-the-art sources suffer from shortcomings in terms of bandwidth, power, size, and complexity, which may require operating at low temperature³⁻⁵ or the presence of optical pumps⁶ and large magnets.

Another fundamental mechanism for generating light, Cherenkov radiation, ^{8–10} has been limited to niche applications, such as medical imaging, dosimetry, and particle detection, because it typically requires highly energetic electrons produced by nuclear reactors, particle accelerators, or radionuclide generators. 11 Recently, lightmatter interactions with photonic quasiparticles¹² and the possibility to obtain Cherenkov radiation in advanced photonic systems has been explored.¹³ For instance, reversed Cherenkov radiation has been studied and experimentally demonstrated in negative-index materials, 13-20 whereas simultaneous forward and backward radiation has been found in photonic crystals.²¹ Additionally, it has been experimentally demonstrated that low-energy electron beams propagating near hyperbolic metamaterials (HMTMs)^{22,23} are able to generate radiation in the visible.²⁴ HMTMs allow control over the electron velocity threshold, intensity, and frequency of the emission by manipulating their anisotropy and local density of states. Other works have also studied this possibility using different structures, such as thin metallic films²⁵ and graphene, 26-28 and unveiled broadband Cherenkov generation exploiting dispersionless plasmons.²¹ The main challenge of all these devices is the need of external electron beams traveling near the nanostructures, which is very difficult to achieve in an integrated fashion. In a related context, it has been predicted that drifting electrons in

a) Author to whom correspondence should be addressed: jsgomez@ucdavis.edu

graphene can couple to surface plasmon polaritons,²⁹ whereas several works have highlighted the coupling between electrons and plasma waves in 2D electron gasses found in transistors and their potential applications.^{30–33} Such processes are somewhat inefficient and narrowband, and thus, it is challenging to apply them to construct sources in practice. Even more recently, drifting electrons in graphene have been shown to enable a plasmonic Doppler effect associated with strong electromagnetic nonreciprocity.^{34–37} In all these platforms, Cherenkov radiation was an afterthought in the sense that it was studied once the electromagnetic properties of the system were fixed, and therefore, it was not possible to manipulate the properties of the resulting radiation.

In this work, we demonstrate that Cherenkov emission can be enforced at desired wavelengths and drastically boosted in terms of efficiency and bandwidth by tailoring at the nanoscale the photonic density of states of the media that surrounds drifting electrons [Fig. 1(a)]. By imposing energy and momentum conservation, we develop an approach to determine the electromagnetic properties of photonic states that allows their excitation from low-energy drifting electrons flowing through the media. Our analytical study reveals that the radiation rate strongly depends on the momentum of the excited photonic states, in terms of (i) magnitude and frequency dispersion and (ii) how it varies with the properties of drifting electrons. These modes can be implemented in practice using a wide variety of photonic configurations, including cavities, resonators, or nanostructures.³⁸ To illustrate this broad concept, we propose to harness emission at long wavelengths by exploiting the coupling between drifting electrons and hyperbolic photonic modes in nanostructures made of 2D materials. Graphene³⁹ is an ideal candidate for this application: it is a highly conductive material whose plasmonic nature at THz/IR

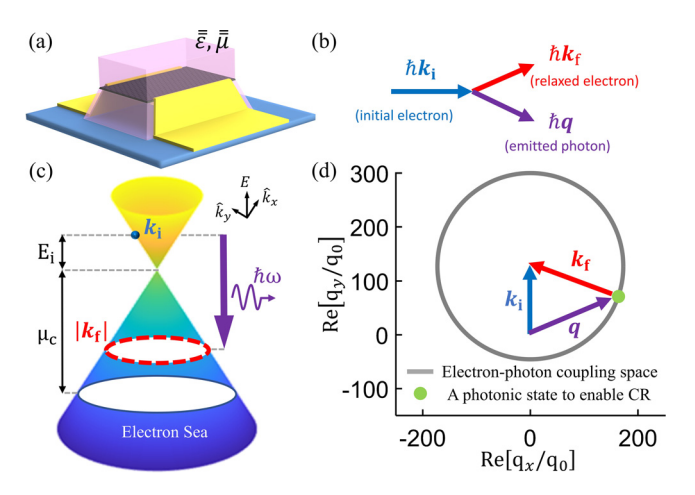


FIG. 1. Tailoring Cherenkov radiation in drift-biased graphene-based nanophotonic devices. (a) Schematic of the structure. Graphene is embedded within an artificial media with effective permittivity and permeability $\bar{\epsilon}$ and $\bar{\mu}$, respectively. (b) Schematic of the emission process. (c) Energy–momentum diagram. A drifting electron in graphene with energy E_i and momentum $k_i = k_y \hat{y}$ spontaneously relaxesy into a state with energy E_f and momentum $|k_f|$ while emitting a photon with energy $\hbar\omega$ and momentum \mathbf{q} . (d) Photonic states of the artificial media that would enable emission at ω (gray line). Any media supporting a state \mathbf{q} within this electron–photon coupling space will enable Cherenkov emission. $\mathbf{q}_0 = \omega/c$ is the free space wavenumber at ω .

frequencies allows hyperbolic modes to be engineered in this range when the material is stacked with dielectrics 40-43 or patterned at the nanoscale. 44-47 Electrons flowing within graphene can be energy- and momentum-matched with broadband yet confined hyperbolic modes to enable a high-rate of photon emission through Cherenkov radiation. Compared to electron–photon coupling in standard plasmonic structures, such as pristine graphene, 29 the use of hyperbolic nanostructures boosts the spontaneous radiation rate over three orders of magnitude and drastically enhances the emission bandwidth to operate from terahertz to mid-IR frequencies. Our theoretical formalism predicts that over 90% of drifting electrons will emit photons, thus opening exciting venues for the development of miniaturized, broadband, and efficient sources.

Let us consider a graphene sheet longitudinally biased with a DC voltage V_{DC} that induces low-energy drifting electrons with velocity $v_d = v_d \hat{y}$ and energy $E_i = \hbar v_F |\mathbf{k_i}|$ [Fig. 1(a)], where \hbar and v_F $\approx 10^6 \mathrm{ms}^{-1}$ are the reduced Planck constant and Fermi velocity, respectively. The goal is to engineer the electromagnetic properties of the media surrounding graphene in terms effective permittivity $(\bar{\bar{\epsilon}})$ and permeability $(\bar{\mu})$ to enforce Cherenkov radiation at a frequency ω [Fig. 1(b)]. This process is illustrated in Fig. 1(c) using an energymomentum diagram: drifting electrons spontaneously relax into states with energy $E_f = \pm \hbar v_F |\mathbf{k}_f|$ and emit photons with momentum \mathbf{q} and energy $\hbar\omega$. The electronic states enabling this process exhibit momenta with magnitude $|\mathbf{k}_f| = |\mathbf{E}_i - \hbar\omega|/\hbar v_F$ that displays a circular shape in the momentum space of Fig. 1(c) [dashed red line in Fig. 1(c)] due to the linear dispersion of graphene. Additionally, graphene's Fermi level μ_c must be lower than the energy of the relaxed states Ef to keep these states vacant. To enable the desired photon emission, the media surrounding drift-biased graphene should support a photonic state q that fulfills momentum conservation, i.e., $\hbar \mathbf{k}_{i} = \hbar \mathbf{k}_{f} + \hbar \mathbf{q}$. Figure 1(d) illustrates this process using an isofrequency (IFC) contour in the photonic momentum space.³⁸ In this diagram, the photonic states that enable Cherenkov emission yield a circle centered at $(0, |\mathbf{k}_i|/q_0)$ and with radius $|\mathbf{k}_f|/q_0$, where q_0 $=\omega/c$ is the free space wavenumber at ω . We denote the momenta of such states as "electron-photon coupling space." Any media that support a state within this space [as the green dot in Fig. 1(d)] would allow spontaneous coupling between drifting electrons and photons through Cherenkov emission. The realm of metamaterials provides large flexibility to engineer artificial media at targeted wavelengths with desired photonic states in the form of bulk waves or even surface plasmon polaritons. Considering a linear, lossless, local, and anisotropic graphene-based metasurface and applying the Fermi's golden rule⁴⁸ as described in the supplementary material, it is possible to analytically calculate the radiation rate into a specific photonic state \mathbf{q}_s as

$$\Gamma_{\mathbf{q}_{s}} = \frac{e^{2}v_{F}}{\pi\hbar^{2}\omega^{2}} \big|\mathbf{E}_{\parallel}\big|^{2} S \frac{d\mathbf{q}_{t}}{d|\mathbf{k}_{f}|} \frac{d\mathbf{q}_{p}}{d\omega} sin^{2} \bigg(\theta - \frac{\pi}{4} - \frac{\varphi}{2}\bigg), \tag{1}$$

where α is the fine structure constant, ω is the photon frequency, ε_0 is the free space permittivity, c is the speed of light, $\theta = \arctan(E_y/E_x)$, $\varphi = \arctan(k_y/k_x)$, $\mathbf{q}_s = \mathbf{q}_t \hat{t} + \mathbf{q}_p \hat{p}$ with \hat{t} and \hat{p} being unit vectors in the direction tangential and perpendicular to the dispersion relation $\mathbf{q}(\omega)$ of the structure evaluated at \mathbf{q}_s , \mathbf{E}_{\parallel} is the in-plane electric field distribution of the photonic state, 49 and $\mathbf{S} \cdot |\mathbf{E}_{\parallel}^2|$ is related to the inplane energy of the excited mode. This formalism is valid for interband transitions—i.e., drifting carriers relaxing from the conduction to the

valence band—and has been expanded in the supplementary material to consider intraband transitions and the presence of loss. Equation (1) reveals that the emission rate depends on the properties of the excited photonic state in terms of energy and momentum. Specifically, it is directly proportional to (i) the frequency dispersion of the supported state and (ii) the variation of the momentum of the excited mode vs the momentum of the relaxed electron—i.e., how the excited state changes as the properties of the drifting carriers evolve. Therefore, it is possible to enforce and manipulate Cherenkov radiation in terms of operation frequency, bandwidth, and efficiency by simultaneously controlling the properties of drifting electrons and the photonic states supported by the surrounding media.

To realize broadband and efficient THz and IR emitters, we propose the unique combination of drifting electrons flowing through graphene and the hyperbolic dispersion of tailored nanostructures. Graphene-based hyperbolic metasurfaces (HMTSs) are excellent candidates for implementing this type of sources as they exhibit a high density of confined photonic states over a broad frequency range in the THz/IR band and can be fabricated by nanostructuring a graphene sheet. 44-47 The design process to construct this type of plasmonic emitters is as follows. First, we consider that electrons with an initial energy E_i are flowing through graphene. In this example, we set a conservative energy of $E_i = 0.03 \, \text{eV} \, (v_d \approx 0.1 \, \text{v}_\text{F})$ —note that drift velocities up to $v_d \approx 0.9 v_F$ have experimentally been reported in graphene encapsulated in hBN.50 The energy of drifting electrons can easily be calculated from its velocity using the Einstein relation. Second, we set graphene's Fermi level well into the valence band ($\mu_c \ll 0 \text{ eV}$) by applying a gate bias, thus providing plenty of empty states in which drifting electrons can relax into. Even though the applied longitudinal bias tilts the Fermi level,⁵¹ this effect is negligible for the drift velocities considered here and does not affect the proposed radiation mechanism. Third, we calculate the electron-photon coupling space vs frequency in the photonic momentum diagram [gray line in Fig. 2(a)]. That space represents the potential photonic states that can be excited in this platform. Other states at desired wavelengths can be obtained by manipulating the initial energy of the flowing electrons. Fourth, we design a hyperbolic metasurface able to support photonic states that intersect with the electron-photon coupling space. Here, we consider an array of densely packed graphene strips with width W = 50 nm and periodicity L = 100 nm. This structure is analyzed using the effective medium theory reported in Ref. 35 that accounts for both, the intrinsic spatial dispersion of graphene and the presence of drifting electrons. The results show that confined and hyperbolic modes are supported over a large bandwidth in the IR [blue line in Fig. 2(a)]. Photonic states excited by drifting electrons are determined by the intersection between the modes supported by the nanostructure and the electron-photon coupling space, as illustrated by magenta lines in Fig. 2(a). The broadband, dispersive, and confined nature of hyperbolic modes permits the generation of photons throughout the IR band (\sim 11 – 30 THz). This is in stark contrast to a common graphene sheet29 in which drifting electrons are unable to efficiently excite broadband photonics modes, as shown in Fig. 2(b). It should be stressed that drift-biased graphene metasurfaces exhibit a nonreciprocal plasmonic response that depends on the drift-velocity of the injected carriers.³⁵ However, the devices proposed here require drifting electrons with limited velocity ($v_d \le 0.1v_F$) that leads to negligible electromagnetic nonreciprocity. Figure 2(c) plots the IFC of the

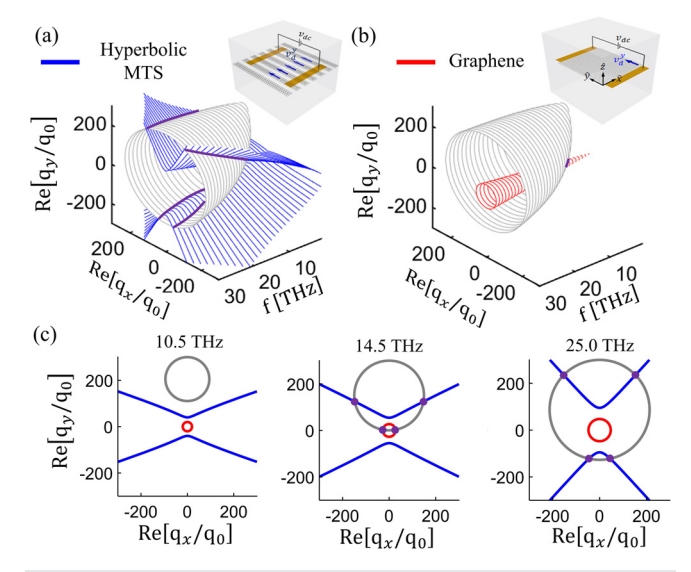


FIG. 2. Photonic momentum diagrams to describe Cherenkov emission in a drift-biased graphene-based hyperbolic metasurface (a) and in a drift-biased graphene layer (b). The panels show the dispersion relation of the devices together with the electron–photon coupling space (gray lines) that would enable radiation. Intersection between supported modes and the electron–photon coupling space (purple lines) indicates the excited photonic states. (c) IFC of the top panels at different frequencies. Graphene's chemical potential is set to $\mu_c=-0.15\,\text{eV}$ and the initial energy of drifting electrons is $E_i=0.03\,\text{eV}$ ($v_d\approx0.1v_F$). The lossless metasurface is composed of an array of packed graphene strips with width $W=50\,\text{nm}$ and periodicity $L=100\,\text{nm}$.

hyperbolic metasurface and graphene sheet together with the electron-photon coupling space. Results show the evolution of the electron-photon coupling space vs frequency. Interestingly, hyperbolic metasurfaces may simultaneously support forward (central panel) and even backward emission (right panel) depending on the momentum of the excited states (magenta dots). Even though emission also appears in a pristine graphene layer, it is very narrowband and inefficient, thus challenging to be observed in practice. In the supplementary material, we further study THz/IR generation in various HMTSs for a wide range of initial energies of the drifting electrons. Our study confirms that the emission is robust, broadband, and can be manipulated with the geometrical parameters that define the nanostructures.

This spontaneous emission process can also be understood using energy-momentum diagrams, as illustrated in Fig. 3 for a HMTS (a) and a graphene sheet (b). Specifically, energy and momentum conservation determine the electronic states in which drifting electrons (blue dot) can relax to. In the case of HMTSs, the electron–photon coupling space translates into a relatively large set of available electronic states that would enable the emission process (solid red line). As a result, a drifting electron has many states to relax to, thus leading to a broadband emission. Note that the distribution of these states as well as the properties of the associated radiation significantly changes with the photonic states supported by the surrounding media. This situation is quite different in the case of a graphene layer because drifting electrons can only relax into a very narrow set of electronic states. As a result, the emission process is narrowband and severely hindered.

Figure 4 shows the total radiation rate and spectrum distribution of the emission predicted in a drift-biased graphene-based HMTS

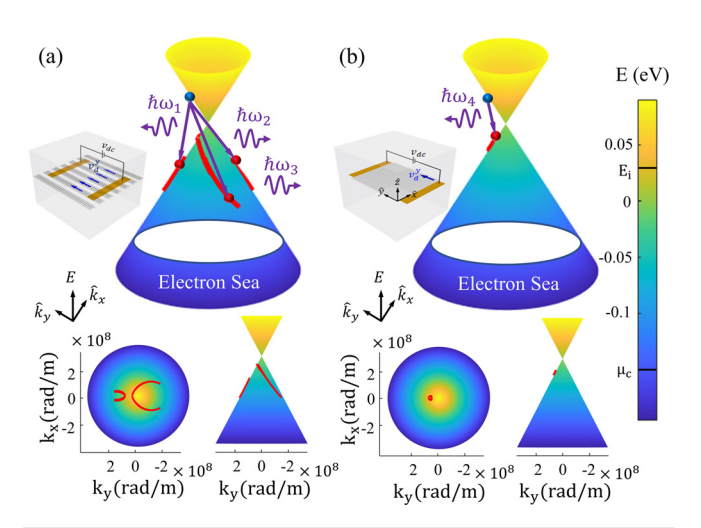


FIG. 3. Electronic energy-momentum diagrams to describe Cherenkov emission in a drift-biased hyperbolic metasurface (a) and in a drift-biased graphene layer (b). Red lines show the allowed states in which drifting electrons (blue ball) can relax into while emitting a photon. Magenta arrows illustrate the emission process for specific cases. Other parameters are as in Fig. 2.

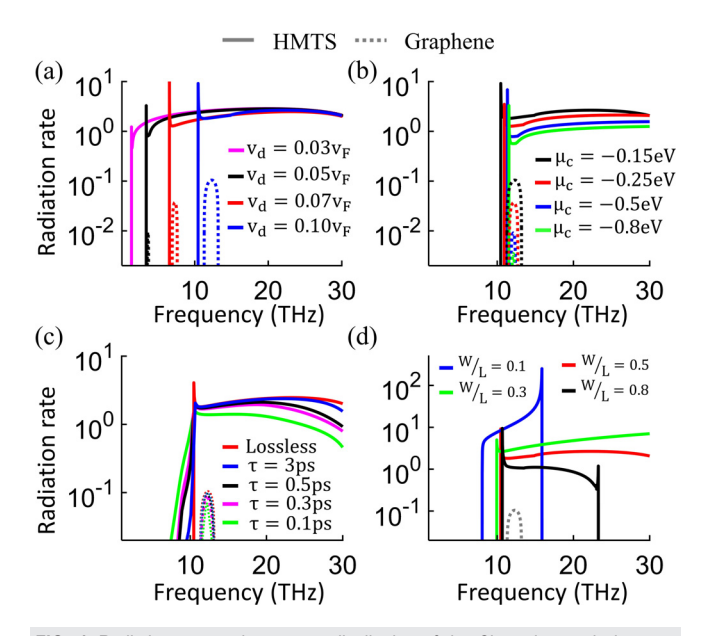


FIG. 4. Radiation rate and spectrum distribution of the Cherenkov emission predicted in the drift-biased hyperbolic metasurface (solid lines) and in the drift-biased graphene layer (dashed lines) described in Fig. 2. Results are plotted vs frequency for different values of the carriers' velocity (a) and properties of the hyperbolic metasurface, including (b) graphene's chemical potential controlled through a gate bias; (c) loss, expressed through graphene's relaxation time τ ; and (d) geometrical dimension of the hyperbolic structure in terms of strip width W over periodicity, L. Values for non-swept parameters are as in Fig. 2.

(solid line) and in a pristine graphene layer (dashed line). Results are computed for a wide range of hyperbolic metasurfaces, accounting for applied gate voltage (i.e., graphene's chemical potential), velocity of drifting carriers, presence of loss (modelled through graphene's

relaxation time), and geometrical dimensions of the strip array (i.e., width and periodicity). It should be noted that the total radiation at a given frequency may be distributed into several photonic states that propagate toward different directions [Fig. 2(c)]. In all cases, the presence of hyperbolic modes drastically boosts the overall efficiency of the emission process compared to the case of pristine graphene²⁹ while simultaneously enhancing the bandwidth from the mid-IR to the THz region. Such response can easily be understood from Eq. (1): hyperbolic modes are more confined than common surface plasmons in graphene and are inherently dispersive, thus leading to a much larger radiation bandwidth. On the one hand, the lower cutoff of the emission is directly proportional to the velocity of the drifting electrons $(f_c \propto v_d)$ and, thus, can easily be manipulated in practice. Figure 4(a) shows that the radiation onset can be tailored to appear at \sim 3 THz by decreasing v_d . It should also be noted that the rate is enhanced close to the emission cutoff frequency, which is attributed to a rapid variation of the coupling between the excited photonic state and drifting electrons [i.e., $dq_t/d|\mathbf{k_f}|$ term in Eq. (1)]. On the other hand, the higher cutoff frequency of the emission is determined by the metasurface topological transition, which in this type of HMTS can be controlled through the geometrical W/L ratio. In case that such topological transition appears at the near-IR band or even shorter wavelengths, phenomena such as interband transitions in graphene's conductivity³⁹ or the metasurface nonlocality⁵² may dominate and determine the radiation cutoff. Our results confirm that the emission rate is resilient against the presence of loss and robust vs variations in the energy of the drifting electrons as well as graphene's quality and doping. The metasurface dispersion relation can be tailored through geometrical parameters (i.e., W/L ratio) to maximize its frequency dispersion, which, in turn, enhances further the radiation rate [Fig. 4(d)]. Optimized geometries provide broadband emission rates over three orders of magnitude compared to the ones found in pristine graphene, an emission level that can be observed in experimental setups. A simple two-state system model^{9,48} permits to characterize this spontaneous emission process and approximately calculate how many drifting electrons will effectively emit photons. Considering a realistic 3 µm long HMTS with made of graphene strips (W/L = 0.5) with relaxation time $\tau = 0.1$ ps that is biased to support drifting electrons with a velocity $v_d = 0.1v_F$, our approach predicts an outstanding efficiency over 90% which is drastically reduced to \sim 0.6% in the case of unpatterned graphene. This efficiency is also larger than the one found in Cherenkov radiation process based on electron beams flowing over graphene nanostructures. 26-28 We attribute such significant increase to the combination of two main mechanisms: a boosted radiation rate due to the enhanced momentum of the hyperbolic states and a large increase in the radiation bandwidth. We note that our study neglects other scattering mechanisms, such electron-electron interactions and phonon excitation. However, we expect these processes to be limited within a timeframe τ . This approximate model highlights the tremendous potential of the proposed platform to develop solid state THz and IR sources.

In conclusion, we have proposed an approach to harness Cherenkov radiation at desired wavelengths by manipulating the photonic states supported by the media surrounding drifting electrons. We have developed an analytical formalism to model this phenomenon in anisotropic metasurfaces that unveils the relation among radiation efficiency, drifting electrons, and the momentum and frequency

dispersion of the supported modes. Rooted on this framework, we have proposed drift-biased graphene-based hyperbolic metasurfaces as a promising candidate to implement plasmonic sources that are (i) broadband, covering from the THz up to the mid-IR frequency range; (ii) highly efficient; (iii) tunable, because the radiation onset is determined by the applied DC voltage; and (iv) miniaturized and easy to realize in practice, as they do not require the presence of optical pumps beams or magnetic fields. Moving beyond, we envision that this concept can be applied to develop a wide variety of solid-state THz and IR sources generating either surface plasmon polaritons or plane waves in free-space. For instance, instead of hyperbolic metasurfaces, such source can rely on bulk graphene-based hyperbolic metamaterials 40-43 realized by alternating layers of graphene and a dielectric. In these structures, drifting electrons flowing inside the device couple to bulk hyperbolic modes that will be subsequently radiated to free-space in the form of plane waves using mechanisms such as diffraction gratings or nanoparticles located at the outer layer. Additionally, configurations such as resonators and cavities can provide the photonic states required to enforce desired radiation, whereas graphene can be substituted by thin layers of gold/silver^{53,54} or other 2D conductive materials, 55,56 thus opening exciting opportunities to construct efficient solid-state THz and IR sources.

See the supplementary material for a detailed description of the proposed quantum formalism, including the development of the radiation rate formula shown in Eq. (1), as well as additional studies regarding the cutoff frequency of the emission and the influence of parameters as graphene's relaxation time and chemical potential, applied bias, geometrical dimensions, and electron velocity on the emission process.

This work was supported by the Keck Foundation and by the National Science Foundation with a CAREER Grant No. ECCS-1749177.

AUTHOR DECLARATIONS Conflict of Interest

The authors have no conflicts to disclose.

Author Contributions

Luqi Wang: Data curation (lead); Formal analysis (lead); Software (lead); Validation (lead); Visualization (lead); Writing – original draft (lead). Nayan K. Paul: Data curation (supporting); Formal analysis (equal); Investigation (supporting); Methodology (supporting); Visualization (supporting); Writing – review & editing (equal). Joshua Hihath: Conceptualization (equal); Funding acquisition (equal); Resources (equal); Supervision (equal); Writing – review & editing (equal). Juan Sebastián Gomez Diaz: Conceptualization (lead); Funding acquisition (lead); Methodology (lead); Supervision (lead); Writing – original draft (supporting); Writing – review & editing (lead).

DATA AVAILABILITY

The data that support this work is available within the article, but if further information is needed, it can be provided from the corresponding author upon request.

REFERENCES

- ¹P. H. Siegel, "Terahertz technology," IEEE Trans. Microwave Theory Tech. 50(3), 910–928 (2002).
- ²M. Tonouchi, "Cutting-edge terahertz technology," Nat. Photonics 1, 97–105 (2007).
- ³J. Faist, F. Capasso, D. L. Sivco *et al.*, "Quantum cascade laser," Science **264**(5158), 553–556 (1994).
- ⁴M. A. Belkin and F. Capasso, "New frontiers in quantum cascade lasers: High performance room temperature terahertz sources," Phys. Scr. **90**(11), 118002 (2015).
- ⁵K. Vijayraghavan, Y. Jiang, M. Jang *et al.*, "Broadly tunable terahertz generation in mid-infrared quantum cascade lasers," Nat. Commun. **4**, 2021 (2013).
- ⁶R. W. Boyd, Nonlinear Optics, 3rd ed. (Academic Press, 2008).
- ⁷J. H. Booske, R. J. Dobbs, C. D. Joye *et al.*, "Vacuum electronic high power terahertz sources," IEEE Trans. Terahertz Sci. Technol. 1, 54–75 (2011).
- ⁸V. L. Ginzburg, "Quantum theory of radiation of electron uniformly moving in medium," Zh. Eksp. Teor. Fiz. **10**, 589–600 (1940).
- ⁹D. Jackson, *Classical Electrodynamics*, 3rd ed. (Wiley, 1998).
- ¹⁰I. Kaminer, M. Mutzafi, A. Levy et al., "Quantum Čerenkov radiation: Spectral cutoffs and the role of spin and orbital angular momentum," Phys. Rev. X 6(1), 011006 (2016).
- ¹¹T. M. Shaffer, E. C. Pratt, and J. Grimm, "Utilizing the power of Cerenkov light with nanotechnology," Nat. Nanotechnol. 12(1), 106–117 (2017).
- ¹²N. Rivera and I. Kaminer, "Light-matter interactions with photonic quasiparticles," Nat. Rev. Phys. 2(10), 538–561 (2020).
- ¹³Z. Su, B. Xiong, Y. Xu et al., "Manipulating Cherenkov radiation and Smith-Purcell radiation by artificial structures," Adv. Opt. Mater. 7, 1801666 (2019).
- ¹⁴V. G. Veselago, "The electrodynamics of substances with simultaneously negative values of ε and μ ," Sov. Phys. Usp. **10**(4), 509–514 (1968).
- ¹⁵J. Lu, T. M. Grzegorczyk, Y. Zhang et al., "Čerenkov radiation in materials with negative permittivity and permeability," Opt. Express 11, 723–734 (2003).
- ¹⁶H. Chen and M. Chen, "Flipping photons backward: Reversed Cherenkov radiation," Mater. Today 14, 34–41 (2011).
- ¹⁷Z. Duan, B.-I. Wu, J. Lu *et al.*, "Cherenkov radiation in anisotropic double-negative metamaterials," Opt. Express 16, 18479–18484 (2008).
- ¹⁸Z. Duan, B.-I. Wu, J. Lu *et al.*, "Reversed Cherenkov radiation in a waveguide filled with anisotropic double-negative metamaterials," J. Appl. Phys. **104**, 063303 (2008)
- ¹⁹S. Xi, H. Chen, T. Jiang *et al.*, "Experimental verification of reversed Cherenkov radiation in left-handed metamaterial," Phys. Rev. Lett. **103**, 194801 (2009).
- ²⁰Z. Duan, X. Tang, Z. Wang *et al.*, "Observation of the reversed Cherenkov radiation," Nat. Commun. 8, 14901 (2017).
- ²¹X. Lin, S. Easo, Y. Shen *et al.*, "Controlling Cherenkov angles with resonance transition radiation," Nat. Phys. 14, 816–921 (2018).
- transition radiation," Nat. Phys. 14, 816–921 (2018).

 22A. Poddubny, I. Iorsh, P. Belov *et al.*, "Hyperbolic metamaterials," Nat. Photonics 7(12), 948–957 (2013).
- ²³V. P. Drachev, V. A. Podolskiy, and A. V. Kildishev, "Hyperbolic metamaterials: New physics behind a classical problem," Opt. Express 21(12), 15048, 15064 (2013)
- ²⁴F. Liu, L. Xiao, Y. Ye, M. Wang *et al.*, "Integrated Cherenkov radiation emitter eliminating the electron velocity threshold," Nat. Photonics 11, 289–292 (2017)
- ²⁵S. Liu, P. Zhang, W. Liu *et al.*, "Surface polariton Cherenkov light radiation source," Phys. Rev. Lett. **109**, 153902 (2012).
- ²⁶S. Liu, C. Zhang, M. Hu, X. Chen et al., "Coherent and tunable terahertz radiation from graphene surface plasmon polaritons excited by an electron beam," Appl. Phys. Lett. 104, 201104 (2014).
- 27C. Yu and S. Liu, "Highly Confined surface plasmon polaritons from graphene quantum Cherenkov effect," Phys. Rev. Appl. 12, 054018 (2019).
- 28X. Zhang, M. Hu, Z. Zhang et al., "High-efficiency threshold-less Cherenkov radiation generation by a graphene hyperbolic grating in the terahertz band," Carbon 183, 225–231 (2021).
- ²⁹I. Kaminer, Y. T. Katan, H. Buljan *et al.*, "Efficient plasmonic emission by the quantum Čerenkov effect from hot carriers in graphene," Nat. Commun. 7(1), ncomms11880 (2016).

- ³⁰M. Dyakonov and M. Shur, "Shallow water analogy for a ballistic field effect transistor: New mechanism of plasma wave generation by dc current," Phys. Rev. Lett. 71, 2465 (1993).
- ⁵¹T. Otsuji, Y. M. Meziani, T. Nishimura et al., "Emission of terahertz radiation from dual grating gate plasmon-resonant emitters fabricated with InGaP/ InGaAs/GaAs material systems," J. Phys.: Condens. Matter 20(38), 384206 (2008).
- ³²F. Veksler, A. P. Teppe, V. Dmitriev *et al.*, "Detection of terahertz radiation in gated two-dimensional structures governed by dc current," Phys. Rev. B 73(12), 125328 (2006).
- ³³M. Dyakonov and M. Shur, "Detection, mixing, and frequency multiplication of terahertz radiation by two-dimensional electronic fluid," IEEE Trans. Electron Devices 43(3), 380–387 (1996).
- 34T. A. Morgado and M. G. Silveirinha, "Negative Landau damping in bilayer graphene," Phys. Rev. Lett 119, 133901 (2017).
- ³⁵⁵D. Correas-Serrano and J. S. Gomez-Diaz, "Nonreciprocal and collimated surface plasmons in drift-biased graphene metasurfaces," Phys. Rev. B **100**(8), 081410(R) (2019).
- 36Y. Dong, L. Xiong, I. Y. Phinney et al., "Fizeau drag in graphene plasmonics," Nature 594, 513–516 (2021).
- ³⁷W. Zhao, S. Zhao, H. Li *et al.*, "Efficient Fizeau drag from Dirac electrons in monolayer graphene," Nature **594**, 517–521 (2021).
- ³⁸B. E. A. Saleh and M. C. Teich, Fundamentals of Photonics, 2nd ed. (Wiley-Interscience, 2007).
- ³⁹ A. H. Castro Neto, F. Guinea, N. M. R. Peres *et al.*, "The electronic properties of graphene," Rev. Mod. Phys. 81(1), 109 (2009).
- ⁴⁰ M. A. K. Othman, C. Guclu, and F. Capolino, "Graphene-based tunable hyper-bolic metamaterials and enhanced near-field absorption," Opt. Express 21(6), 7614–7632 (2013).
- ⁴¹I. V. Iorsh, I. S. Mukhin, I. V. Shadrivov *et al.*, "Hyperbolic metamaterials based on multilayer graphene structures," Phys. Rev. B 88(7), 075416 (2013).
- ⁴²J. Brouillet, G. Papadakis, and H. Atwater, "Experimental demonstration of tunable graphene-polaritonic hyperbolic metamaterial," Opt. Express 27(21), 30225–30232 (2019).

- ⁴³Y. C. Chang, C. H. Liu, C. H. Liu *et al.*, "Realization of mid-infrared graphene hyperbolic metamaterials," Nat. Commun. 7(1), 10568 (2016).
- ⁴⁴J. S. Gómez-Díaz, M. Tymchenko, and A. Alù, "Hyperbolic plasmons and topological transitions over uniaxial metasurfaces," Phys. Rev. Lett. **114**(23), 233901 (2015).
- 45J. S. Gomez-Diaz and A. Alù, "Flatland optics with hyperbolic metasurfaces," ACS Photonics 3(12), 2211–2224 (2016).
- ⁴⁶E. Yoxall, M. Schnell, A. Y. Nikitin *et al.*, "Direct observation of ultraslow hyperbolic polariton propagation with negative phase velocity," Nat. Photonics 9(10), 674–678 (2015).
- ⁴⁷P. Li, I. Dolado, F. J. Alfaro-Mozaz, F. Casanova et al., "Infrared hyperbolic metasurface based on nanostructured van der Waals materials," Science 359, 892–896 (2018).
- ⁴⁸R. Shankar, *Principles of Quantum Mechanics*, 1st ed. (Springer Science & Business Media, 2012).
- ⁴⁹D. Correas-Serrano, A. Alù, and J. S. Gómez-Díaz, "Plasmon canalization and tunneling over anisotropic metasurfaces," Phys. Rev. B 96(7), 075436 (2017).
- 50 M. A. Yamoah, W. Yang, and E. Pop, "High-velocity saturation in graphene encapsulated by hexagonal boron nitride," ACS Nano 11(10), 9914–9919 (2017)
- ⁵¹B. V. Duppen, A. Tomadin, A. N. Grigorenko *et al.*, "Current-induced birefringent absorption and non-reciprocal plasmons in graphene," 2D Mater. 3, 015011 (2016).
- ⁵²D. Correas-Serrano, J. S. Gómez-Díaz, M. Tymchenko et al., "Nonlocal response of hyperbolic metasurfaces," Opt. Express 23(23), 29434–29448 (2015).
- ⁵³K. Y. Bliokh, F. Rodríguez-Fortuño, A. Y. Bekshaev et al., "Electric-current-induced unidirectional propagation of surface plasmon-polaritonsm," Opt. Lett. 43(5), 963–966 (2018).
- ⁵⁴R. A. Maniyara, D. Rodrigo, R. Yu et al., "Tunable plasmons in ultrathin metal films," Nat. Photonics 13(5), 328–333 (2019).
- 55S. Manzeli, D. Ovchinnikov, D. Pasquier et al., "2D transition metal dichalcogenides," Nat. Rev. Mater. 2(8), 17033 (2017).
- 56D. Akinwande, C. Huyghebaert, C. H. Wang et al., "Graphene and two-dimensional materials for silicon technology," Nature 573, 507–518 (2019).